Electronic Supplementary Material (ESI) for Chemical Communications.

Electronic Supplementary Material for

Nitric Oxide Release via Oxygen Atom Transfer from Nitrite at Copper(II)

Zeinab Sakhaei, Subrata Kundu, Jane M. Donnelly, Jeffery A. Bertke, William Y. Kim, and
Timothy H. Warren*

Department of Chemistry, Georgetown University, Box 571227, Washington, D. C., 20057-1227,
United States.

*Corresponding author email: thw@georgetown.edu

Table of Contents **S1**

1. Instrumentation and Physical Methods.

Preparation and handling of air-sensitive chemicals were done under dry nitrogen atmosphere by utilizing MBraun glove-boxes and/or standard Schlenk techniques. ^{1}H, ^{13}C, and ^{19}F NMR spectra were obtained on a Varian 400 MHz spectrometer at room temperature (RT) unless otherwise noted. ^{31}P NMR spectra were recorded on a Varian 121 MHz spectrometer at RT. ^{1}H and ^{13}C chemical shift were reported as δ values downfield from the internal standard tetramethylsilane. ^{19}F NMR spectra were recorded at 376 MHz using an internal reference of C_6H_5-CF_3 (δ = -63.72 ppm). ^{31}P chemical shifts were referenced relative to an internal standard of bis(4-fluorophenyl)phenylphosphine oxide (δ = 23.91 ppm), which was referenced to external standard of H_3PO_4 in deuterated water (δ = 0.00). ^{15}N NMR spectra were referenced to external standard $Na^{15}NO_2$ in D_2O (609.5 ppm vs liquid NH_3). Elemental analyses were performed on a Perkin-Elmer PE2400 micro-analyzer at Georgetown University. UV-vis spectra were recorded either on a Cary 50 dual beam or Agilent 8454 Diode Array spectrometer equipped with stirrer and Unisoku USP-203 cryostats for variable temperature (-105 °C to 90 °C) experiments. The molar extinction coefficients of different isolated complexes were determined from the Beer's law plot (absorbance *vs* concentration) with at least four different concentrations. IR spectra (with spectral resolution of 2 cm^{-1}) were collected on a Varian 3100 FT-IR spectrometer by using KBr pellet method. The intensities of the vibrational bands are abbreviated as follows: s = strong, m = medium, w = weak, br = broad. The EPR measurements were performed in air-tight quartz tubes. EPR spectra were recorded on a JEOL continuous wave spectrometer JES-FA200 equipped with an X-band Gunn oscillator bridge, a cylindrical mode cavity, and a liquid nitrogen cryostat. EPR measurements were performed in sealed quartz tubes and the simulation of EPR spectra were carried out using the program QCMP 136 by Prof. Dr. Frank Neese from the Quantum Chemistry Program Exchange as described by Neese *et al.* in *J. Am. Chem. Soc.* **1996**, *118*, 8692-8699. Cyclic voltammetry measurements were carried out at RT under dry nitrogen atmosphere using BASi Epsilon Potentiostat. A three-electrode system was used and consisted of a glassy carbon working electrode, high surface area platinum coil counter electrode, and a BASI non-aqueous reference electrode (MF-2062) containing a silver wire immersed in a 0.01 M $AgNO_3$.

2. Materials.

All chemicals were purchased from regular vendors (e.g. Sigma-Aldrich, Acros Organics, Strem Chemicals, TCI) and used without further purification unless otherwise mentioned. Molecular sieves (4 Å, 4-8 mesh beads) were obtained from Fisher Scientific and activated in *vacuo* at 180 °C for 24 h. Extra dry solvents (≥99.5%) with Acroseal® and deuterated solvents were purchased from Acros Organics and Cambridge Isotope Laboratories, respectively. Both anhydrous and deuterated solvents were sparged with nitrogen and stored over activated molecular sieve under nitrogen atmosphere. (TPP)Co was purchased from Strem Chemicals.

$Ag^{15}NO_2$ was prepared using commercially available $Na^{15}NO_2$ (98+ atom% ^{15}N from Cambridge Isotope Laboratories) and by following the previously published procedure.[1] A solution of $AgNO_3$ (1.91 g, 11.2 mmol) in 5.0 mL of distilled water was added slowly to a vigorously stirring solution of $Na^{15}NO_2$ (0.79 g, 11.2 mmol) in 3 mL of distilled water. A faint yellow precipitate of $Ag^{15}NO_2$ immediately precipitated out of the solution. The resultant mixture was allowed to stand in the dark for 1 h. The yellow precipitate was collected by suction filtration and washed thoroughly with distilled water and methanol. The product was dried under high vacuum to afford $Ag^{15}NO_2$ as a yellow powder (1.41 g, 9.1 mmol). The product was characterized by comparing the FT-IR spectra of the commercially available $AgNO_2$ (from Strem Chemicals). FT-IR (KBr pellet, cm^{-1}): 848 (^{14}N), 840 (^{15}N).

$[Bu_4N]^{15}NO_2$ was prepared from the reaction of $[Bu_4N]Br$ and $Ag^{15}NO_2$. A solution of $[Bu_4N]Br$ (1.97 g, 6.10 mmol) in 3 mL anhydrous THF was added to a stirring solution of $Ag^{15}NO_2$ (0.94 g, 6.10 mmol) in THF. The mixture was allowed to stir for 2 h. The resultant light green solution was evaporated under reduced pressure to afford the desired product as a yellow powder in 0.42 g (76%).

3. Synthesis and Characterization of [^{i}Pr$_2$NN$_{F6}$]H.

The ligand [^{i}Pr$_2$NN$_{F6}$]H was synthesized by a slight modification of a previously reported procedure.[2] Under nitrogen atmosphere, titanium tetrachloride (19.9 g, 105 mmol, 11.5 mL) was added drop-wise to a vigorously stirring solution of 2,6-diisopropyloroaniline (53.2 g, 300 mmol) in anhydrous heptane (250 mL). A dense orange precipitate was formed immediately. After stirring the reaction mixture for 2 hours at RT, 1,1,1,5,5,5-hexafluoro-2,4-pentanedione (10.4 g, 50 mmol, 7 mL) was added to the previous solution. The resultant reaction mixture was refluxed overnight at 130 °C. The color of the reaction mixture turned light yellow with a significant amount of precipitate consisting of titanium dioxide and 2,6-diisopropylanilinium chloride. The yellow solution was isolated by suction filtration and water/pentane extraction was employed for work up. The orange-yellow organic phase thus obtained was treated with anhydrous $MgSO_4$ and the solvent was removed under reduced pressure to afford a yellow oily mass. The product was dissolved in methanol (100 mL) and left at -20 °C overnight to isolate the desired product as shiny yellow crystals (2.5 g, 4.7 mmol). Yield: 10%. ^{1}H NMR (400 MHz, C_6D_6): δ 1.04 (d, 12H, Ar-CH-(C*H*$_3$)$_2$), 1.22 (d, 12H, Ar-CH-(C*H*$_3$)$_2$), 3.09 (m, 4H, Ar-C*H*-(CH$_3$)$_2$), 6.02 (s, 1H, backbone-C*H*), 7.06 (d, 4H, *m*-Ar-*H*), 7.12 (d, 2H, *p*-Ar-*H*), 11.55 (s, 1H, -N*H*). ^{19}F NMR (376 MHz, C_6D_6): δ -65.29 (s, -C*F*$_3$).

4. Synthesis and Characterization of $[{}^{i}\mathrm{Pr}_2\mathrm{NN}_{\mathrm{F6}}]\mathrm{Cu}(\eta^2\text{-benzene})$ (1).

A two-step synthesis (Scheme S1) was employed.

Scheme S1. Synthesis of $[{}^{i}\mathrm{Pr}_2\mathrm{NN}_{\mathrm{F6}}]\mathrm{Cu}(\eta^2\text{-benzene})$ (**1**).

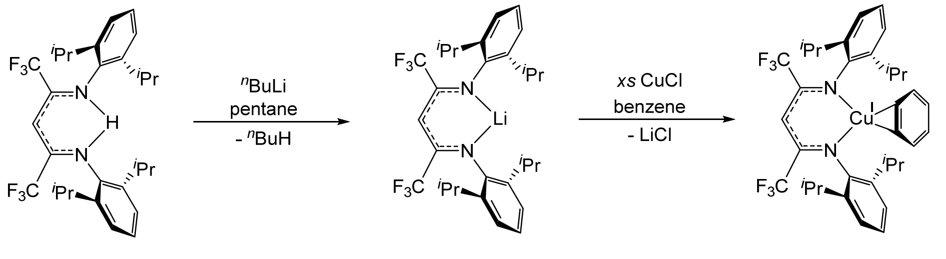

$[{}^{i}\mathrm{Pr}_2\mathrm{NN}_{\mathrm{F6}}]\mathrm{H}$ $[{}^{i}\mathrm{Pr}_2\mathrm{NN}_{\mathrm{F6}}]\mathrm{Li}$ $[{}^{i}\mathrm{Pr}_2\mathrm{NN}_{\mathrm{F6}}]\mathrm{Cu}(\eta^2\text{-benzene})$ (**1**)

Step 1: To a chilled solution of $[{}^{i}\mathrm{Pr}_2\mathrm{NN}_{\mathrm{F6}}]\mathrm{H}$ (2.56 g, 4.86 mmol) in anhydrous pentane (10 mL), 1.5 equivalent of ^{n}BuLi (2.92 mL of 2.5 M ^{n}BuLi in hexane, 7.3 mmol) was added drop-wise and the reaction mixture was stirred at RT for 3 h. The pale yellow precipitate thus obtained was isolated on a filter frit and washed thoroughly with pentane to remove unreacted ligand and/or ^{n}BuLi. The lithium salt of the ligand $[{}^{i}\mathrm{Pr}_2\mathrm{NN}_{\mathrm{F6}}]\mathrm{Li}$ was dried under vacuum to obtain a pale yellow powder in near quantitative yield.

Step 2: A suspension of $[{}^{i}\mathrm{Pr}_2\mathrm{NN}_{\mathrm{F6}}]\mathrm{Li}$ (2.66 g, 4.99 mmol) and ~5 equivalents of anhydrous CuCl (2.47 g, 24.95 mmol) in anhydrous benzene (~20 mL) was stirred at RT for 16 h. Due to the poor solubility of both the lithium salt $[{}^{i}\mathrm{Pr}_2\mathrm{NN}_{\mathrm{F6}}]\mathrm{Li}$ and CuCl in benzene, 5 equivalents of CuCl was required to afford the desired product in optimum yield. The resultant reaction mixture was filtered through Celite to remove the insoluble residue and the dark brownish-yellow filtrate, which was evaporated under reduced pressure to obtain the desired product as an orange-yellow microcrystalline powder **1** in 2.49 g (75%) yield. ^{1}H NMR spectra demonstrates the formation of a copper(I) complex. ^{1}H NMR (400 MHz, $\mathrm{C_6D_6}$): δ 0.97 (d, 12H, Ar-CH-(C*H*$_3$)$_2$), 1.11 (d, 12H, Ar-CH-(C*H*$_3$)$_2$), 2.91 (m, 4H, Ar-C*H*-(CH$_3$)$_2$), 5.86 (s, 1H, backbone-C*H*), 7.10 (s, 6H, Ar-*H*). ${}^{13}\mathrm{C}\{{}^{1}\mathrm{H}\}$ NMR (100 MHz, $\mathrm{C_6D_6}$): δ NMR (100 MHz, 298 K, $\mathrm{C_6D_6}$): δ 152.92 (q, ${}^{2}J_{\mathrm{CF}}$ = 25.7 Hz), 146.10, 139.26, 128.59, 124.94, 123.85, 121.96 (q, ${}^{1}J_{\mathrm{CF}}$ = 288.5 Hz), 85.33 (m, ${}^{3}J_{\mathrm{CF}}$ = 4.0 Hz), 28.61, 24.26, 24.07. ^{19}F NMR (376 MHz, $\mathrm{C_6D_6}$): δ -60.89 (s, -C*F*$_3$). Elemental analysis: calculated for $\mathrm{C_{35}H_{41}F_6N_2Cu}$: C, 63.00; H, 6.19; N, 4.20. Found: C, 63.10; H, 6.23; N, 4.30.

5. Synthesis and Characterization of $[Bu_4N]\{[^{i}Pr_2NN_{F6}]Cu(\kappa^1\text{-}NO_2)\}$ (2). A mixture of **1** (0.94 g, 1.4 mmol) and 1 equiv. $[Bu_4N]NO_2$ (0.41 g, 1.4 mmol) in anhydrous THF (~10 mL) was stirred at RT for 4 h. The resultant red precipitate was isolated on a filter frit and washed thoroughly with pentane. The precipitate was dried under reduced pressure to afford the **2** as a red powder (0.92 g, 75% yield). ^{1}H NMR (400 MHz, C_6D_6): δ 0.72 (t, 12H, N-$(CH_2)_3$-C*H*$_3$), 0.86 (m, 16H, N-CH_2-(C*H*$_2$)$_2$-CH_3), 1.47 (d, 12H, Ar-CH-(C*H*$_3$)$_2$), 1.79 (d, 12H, Ar-CH-(C*H*$_3$)$_2$), 2.33 (t, 8H, N-C*H*$_2$-C_3H_7), 3.69 (sp, 4H, Ar-C*H*-$(CH_3)_2$), 6.26 (s, 1H, backbone-C*H*), 7.03 (t, 2H, *p*-Ar-*H*), 7.18 (d, 4H, *m*-Ar-*H*), ^{13}C{^{1}H} NMR (100 MHz, C_6D_6): δ 150.37 (q, $^2J_{CF}$ = 24.0 Hz), 146.44, 140.31, 123.87, 122.73, 121.9 (q, $^1J_{CF}$ = 288.1 Hz), 82.92 (m, $^3J_{CF}$ = 4.7 Hz), 58.14, 28.95, 25.56, 23.65, 23.40, 19.65, 13.68. ^{19}F NMR (376 MHz, C_6D_6): δ -62.21 (s, -C*F*$_3$). Elemental analysis: calculated for $C_{45}H_{71}F_6N_4O_2Cu$: C, 61.59; H, 8.15; N, 6.38. Found: C, 61.69; H, 8.08; N, 6.38. FT-IR (KBr pellet, cm^{-1}): 2960m, 1479s, 1363w, 1309m, 1294s, 1178m, 1170s, 1132m, 1093m, 955w, 871w.

$[Bu_4N]\{[^{i}Pr_2NN_{F6}]Cu(\kappa^1\text{-}^{15}NO_2)\}$ (2-^{15}N) was prepared with $[Bu_4N]^{15}NO_2$ and **1**. ^{15}N NMR (41 MHz, THF-d_8): δ 512 ppm.

6. Synthesis and Characterization of [^{i}Pr$_2$NN$_{F6}$]Cu(κ^2-O$_2$N) (3).

A mixture of **1** (1.34 g, 2.01 mmol) and 2.4 equiv. AgNO$_2$ (0.74 g, 4.83 mmol) in anhydrous fluorobenzene (~10 mL) was stirred at RT for 2 h. The resultant dark green reaction mixture was filtered through Celite to remove the insoluble residue. The dark green filtrate thus obtained was evaporated under reduced pressure to afford the desired product as a green powder **3** in 1.02 g (80%) yield. To obtain higher purity, the product was recrystallized from pentane at -40 °C. Elemental analysis: calculated for $C_{29}H_{35}F_6N_3O_2Cu$: C, 54.84; H, 5.55; N, 6.62. Found: C, 54.84; H, 5.73; N, 6.60. UV-Vis (pentane, 25 °C): λ_{max} = 615 nm (ε = 500 M^{-1}cm^{-1}), 440 nm (ε = 1440 M^{-1}cm^{-1}). FT-IR (KBr pellet, cm^{-1}): 2968m, 2873w, 2360m, 1560m, 1442s, 1321m, 1290m, 1244m, 1209s, 1157br, 1095m, 887w, 794s.

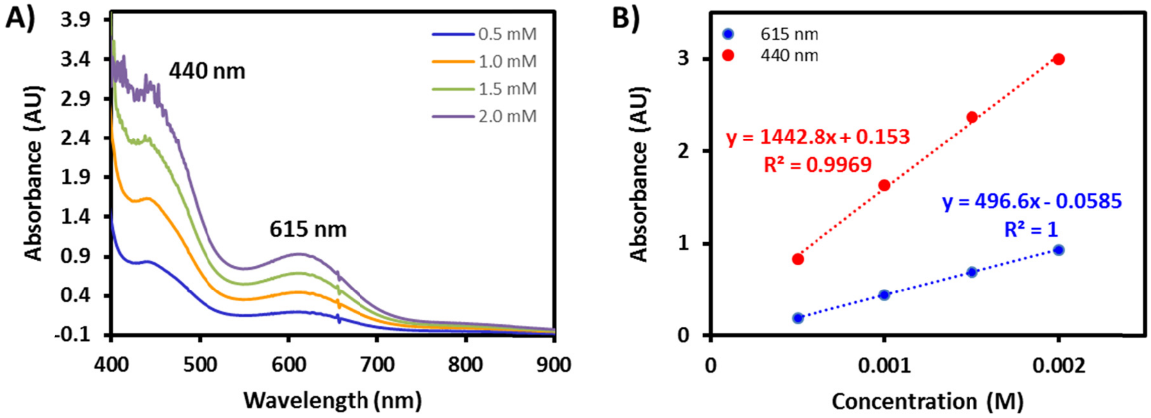

Figure S1. A) UV-Vis spectra of **3** in pentane at 25 °C at different concentrations. B) Beer's law plot for **3** depicts λ_{max}/nm (ε/M^{-1}cm^{-1}) = 440 (1440), 615 (500).

[^{i}Pr$_2$NN$_{F6}$]Cu(κ^2-O$_2$^{15}N) (3-^{15}N) was prepared from Ag^{15}NO$_2$ and **1**. The 887 cm^{-1} band in the IR spectrum of **3** shifts to 881 cm^{-1} upon substitution with ^{15}NO$_2$ in **3-^{15}N**.

7. Synthesis and Characterization of $\{[^{i}Pr_2NN_{F6}]Cu\}_2(\mu\text{-}\kappa^2\text{:}\kappa^1\text{-}NO_2)$ (4).

Procedure 1: A mixture of **1** (157.3 mg, 0.24 mmol) and 1 equiv. **3** (150 mg, 0.24 mmol) in anhydrous fluorobenzene (~10 mL) was stirred at RT for 2 h. The resultant dark red solution was dried under reduced pressure to afford **4** as a dark red powder in 220.4 mg (75%) yield. X-ray quality crystals were grown from fluorobenzene at -40 °C. Elemental analysis: calculated for $C_{58}H_{70}F_{12}N_5Cu_2 \cdot 0.65\ C_6H_5F$: C, 57.78; H, 5.74; N, 5.44. Found: C, 58.02; H, 6.04; N, 5.39. 4 equiv. fluorobenzene / **4** appears in the X-ray structure of **4**. We have not been able to obtain elemental analysis consistent with full (or without) solvent occupancy. UV-Vis (pentane, 25 °C): λ_{max} = 650 nm (ε = 1130 $M^{-1}cm^{-1}$), 508 nm (ε = 3200 $M^{-1}cm^{-1}$). FT-IR (KBr pellet, cm^{-1}): 2962m, 1552m, 1466s, 1363w, 1325s, 1213s, 1172s, 1097m, 877m.

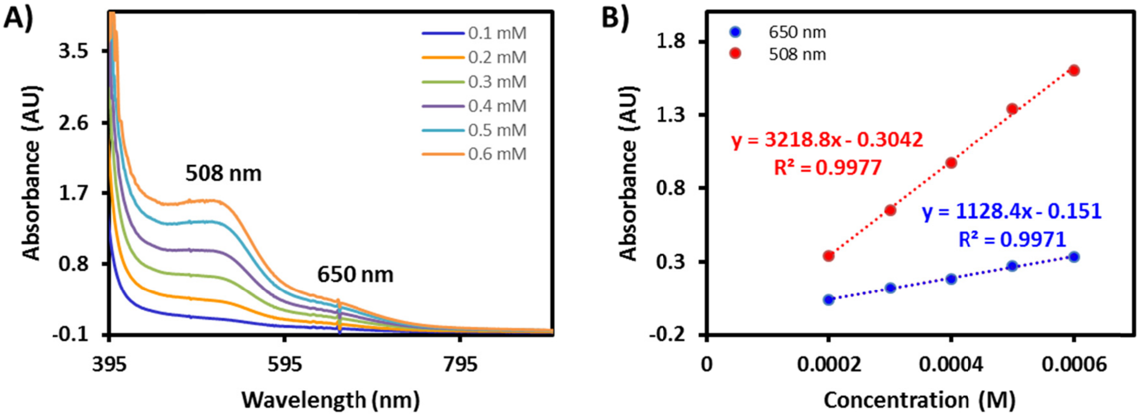

Figure S2. A) UV-Vis spectra of **4** in pentane at 25 °C at different concentrations. B) Beer's law plot for **4** depicts λ_{max}/nm (ε/$M^{-1}cm^{-1}$) = 508 (3200), 650 (1130).

$\{[^{i}Pr_2NN_{F6}]Cu\}_2(\mu\text{-}\kappa^2\text{:}\kappa^1\text{-}NO_2)$ (4-^{15}N) was prepared from **3-^{15}N** and **1**. The 879 cm^{-1} band in the IR spectrum of **4** shifts to 873.8 cm^{-1} upon substitution with $^{15}NO_2$ in **4-^{15}N**.

Procedure 2: {[^{i}Pr$_2$NN$_{F6}$]Cu}$_2$(μ-κ^2:κ^1-NO$_2$) **(4)** can be independently prepared the reaction of **1** and 2-4 equivalents of nitric oxide (NO). A solution of **1** (200 mg, 0.30 mmol) in anhydrous fluorobenzene was bubbled with NO (22 mL, 0.90 mmol). The resultant dark red solution was dried under reduced pressure to afford **4** as a dark red powder in 160 mg (80%) yield. The product was dissolved in anhydrous pentane and left at -40 °C overnight to afford single crystals of **4** suitable for X-ray spectroscopy.

For the detection of additional nitrogen oxide coproducts ^{15}N NMR spectrum of a sample enriched with ^{15}N isotope was analyzed. A solution of **1** (53.0 mg, 0.079 mmol) in toluene-d$_8$ was taken in a J Young NMR tube and cooled to -40 °C. 2 equiv. of ^{15}NO (*ca.* 2 mL, 1.0 atm) was added to the chilled solution of **1**. The resultant dark reddish-purple solution was examined by ^{15}N NMR spectroscopy.

Scheme S2. Synthesis of {[^{i}Pr$_2$NN$_{F6}$]Cu}$_2$(μ-κ^2:κ^1-NO$_2$) (**4**) from **1** and NO$_{(g)}$.

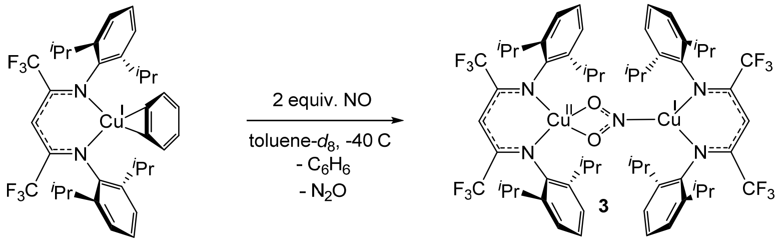

[^{i}Pr$_2$NN$_{F6}$]Cu(η^2-benzene) (**1**)

{[^{i}Pr$_2$NN$_{F6}$]Cu}$_2$-(μ–κ^2:κ^1-NO$_2$) (**4**)

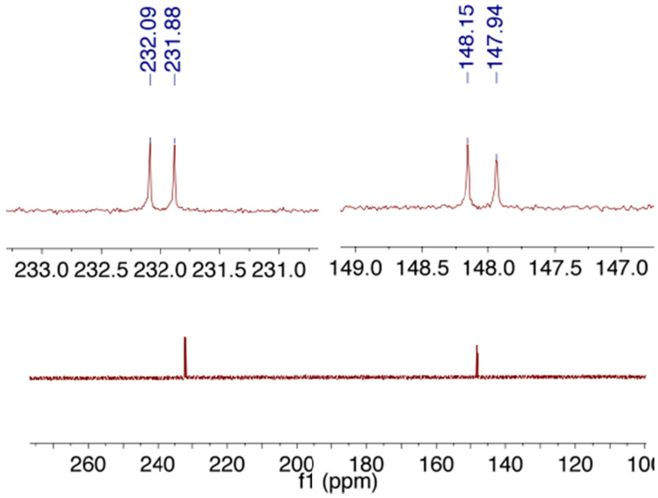

Figure S3. ^{15}N NMR spectrum (41 MHz, toluene-d_8, RT) of the crude mixture obtained from the reaction of **1** and two equiv. of ^{15}NO$_{(g)}$. Insets show the zoomed spectra of each doublet. Two peaks at $\delta = 232.0$ (d, $^1J_{NN} = 8.61$ Hz) and 148.0 (d, $^1J_{NN} = 8.61$ Hz) appears from two inequivalent nitrogen atoms in ^{15}N$_2$O.

8. Synthesis and Characterization of [^{i}Pr$_2$NN$_{F6}$]Cu(PPh$_3$) (5).

A mixture of **1** (100.5 mg, 0.15 mmol) and 1 equiv. PPh$_3$ (39.6 mg, 0.15 mmol) in anhydrous fluorobenzene (~2 mL) was stirred at RT for 0.5 h. The solution was then layered with anhydrous pentane to afford orange crystals. Crystals were dried under reduced pressure to afford **5** (110 mg, 50% yield). ^{1}H NMR (400 MHz, C_6D_6): δ 0.73 (d, 12H, Ar-CH-(C*H*$_3$)$_2$), 1.27 (d, 12H, Ar-CH-(C*H*$_3$)$_2$), 3.41 (sp, 4H, Ar-C*H*-(CH$_3$)$_2$), 6.24 (s, 1H, backbone-C*H*), 6.8 (m, 13H, Ar-*H*), 6.93 (m, 6H, Ar-*H*), 7.02 (t, 2H, *m*-Ar-*H*). ^{13}C{^{1}H} NMR (100 MHz, C_6D_6): δ 153.41 (qd, $^2J_{CF}$ = 26.0 Hz, $^3J_{CP}$ = 2.0 Hz), 147.72, 140.20, 133.71 (d, $^3J_{CP}$ = 14.0 Hz), 132.49 (d, $^1J_{CP}$ = 39.0 Hz), 129.87 (d, $^4J_{CP}$ = 2.0 Hz), 129.01 (d, $^3J_{CP}$ = 10.0 Hz), 125.17, 123.98, 122.25 (qd, $^1J_{CF}$ = 289.0 Hz, $^4J_{CP}$ = 2.0 Hz), 115.51 (d, $^2J_{CP}$ = 21.0 Hz), 86.76 (m, $^3J_{CF}$ = 4.26 Hz, $^4J_{CP}$ = 1.3 Hz), 28.71, 24.64, 24.15. ^{19}F NMR (376 MHz, C_6D_6): δ -60.42 (s, -C*F$_3$*). ^{31}P NMR (121 MHz, C_6D_6): δ 0.18 (s, PPh$_3$). Elemental analysis: calculated for $C_{47}H_{50}F_6N_2PCu$: C, 66.30; H, 5.92; N, 3.29. Found: C, 66.16; H, 6.04; N, 3.28.

9. Synthesis and Characterization of [^{i}Pr$_2$NN$_{F6}$]Cu(CNAr) (6).

A mixture of **1** (103.4 mg, 0.15 mmol) and 1 equiv. 2,6-dimethylphenyl isocyanide (20.3 mg, 0.15 mmol) in anhydrous fluorobenzene (~2 mL) was stirred at RT for 0.5 h. The solution was then layered with anhydrous pentane to afford orange crystals. Crystals were dried under reduced pressure to afford the highly soluble **6** (23 mg, 21% yield). ^{1}H NMR (400 MHz, C_6D_6): δ 1.34 (t, 24H, Ar-CH-(C*H*$_3$)$_2$), 1.56 (s, 6H, Ar-C*H*$_3$), 3.34 (m, 4H, Ar-C*H*-(CH$_3$)$_2$), 6.26 (s, 1H, backbone-C*H*), 6.36 (d, 2H, *m*-Ar-*H*), 6.58 (t, 1H, *p*-Ar-*H*), 7.09 (m, 6H, Ar-*H*). ^{13}C{^{1}H} NMR (100 MHz, C_6D_6): δ 146.88, 139.94, 135.33, 125.08, 123.21, 58.67, 28.72, 25.45, 24.30, 22.73, 20.17, 18.24, 14.03. The ligand backbone ^{13}C resonances were not observed due to C-F coupling. ^{19}F NMR (376 MHz, C_6D_6): δ -64.18 (s, -C*F$_3$*). Elemental analysis: calculated for $C_{38}H_{44}F_6N_3Cu$: C, 63.36; H, 6.16; N, 5.83. Found: C, 63.86; H, 6.55; N, 5.92. FT-IR (KBr pellet, cm^{-1}): 2962m, 2144s (ν_{CN}), 1541m, 1464s, 1323s, 1211m, 1170s, 1095m, 1057w, 777s.

10. Reaction of [^{i}Pr$_2$NN$_{F6}$]Cu(κ^2-O$_2$N) (3) with PPh$_3$ and CNAr (Ar = 2,6-Me$_2$C$_6$H$_3$).

i. Reaction of [^{i}Pr$_2$NN$_{F6}$]Cu(κ^2-O$_2$N) (3) with PPh$_3$.

To a solution of **3** in C_6D_6 (2.0 mL of 15mM solution, 0.03 mmol), was added a C_6D_6 solution containing 2 equiv. PPh$_3$ (0.5 mL of 120 mM solution, 0.06 mmol). A trifluorotoluene standard was also added (1 equiv). There was no immediate color change but gas was evolved (for gas trapping experiments see Section 12). After 4 hours stirring, the resultant solution was analyzed by ^{19}F NMR spectroscopy, which exhibits the formation of **5** in 93% yield as judged by the resonance at δ -60.42 ppm. Detection of OPPh$_3$ is achieved via ^{31}P NMR spectroscopy. The difference between the yields of formation of **5** in ^{19}F NMR versus ^{31}P NMR, as well as the yield of OPPh$_3$ formation is indicative of the high reactivity of NO towards excess PPh$_3$ to form OPPh$_3$ and N_2O.[3] ^{19}F NMR spectrum (376 MHz, C_6D_6): *δ* -60.42 (s, -C*F*$_3$, compound **5**). ^{1}H NMR (400 MHz, C_6D_6): δ 0.73 (d, 12H, Ar-CH-(C*H*$_3$)$_2$, compound **5**), 1.27 (d, 12H, Ar-CH-(C*H*$_3$)$_2$, compound **5**), 3.40 (m, 4H, Ar-C*H*-(CH$_3$)$_2$, compound **5**), 6.24 (s, 1H, backbone-C*H*, compound **5**). ^{31}P NMR spectrum (121 MHz, C_6D_6): *δ* -8.36 (s, *P*Ph$_3$ unreacted), -0.74 (s, compound **5**), 20.99 (s, O*P*Ph$_3$).

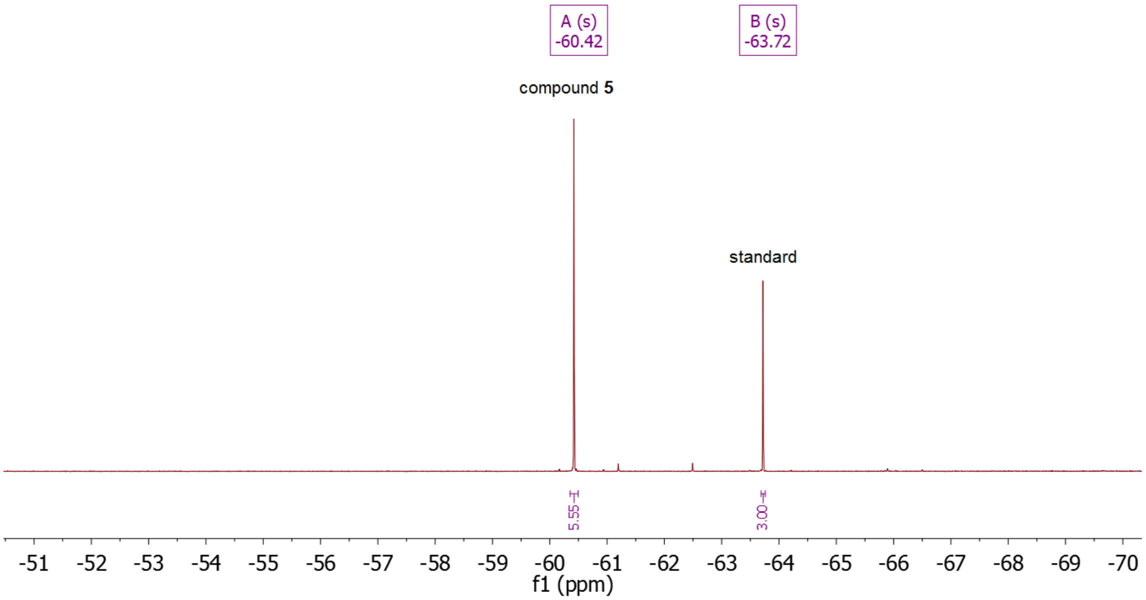

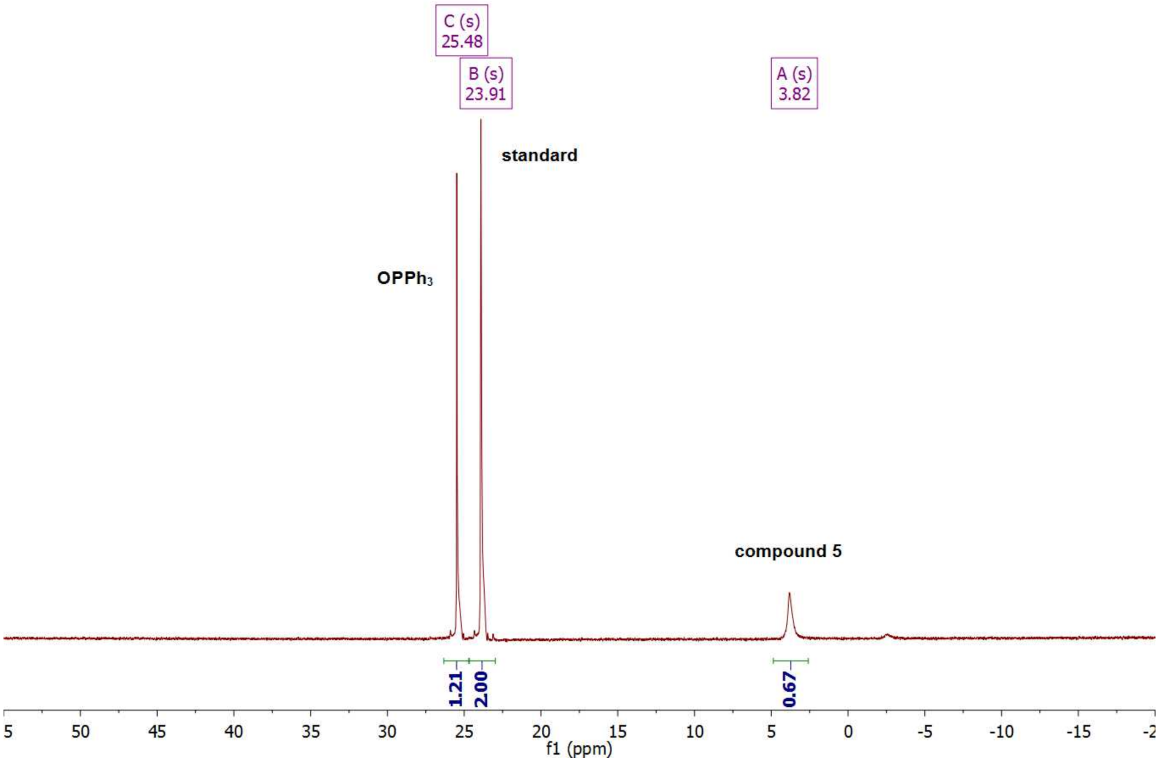

Figure S4. (top) ^{19}F NMR spectrum (376 MHz, C_6D_6); (bottom) ^{31}P NMR spectrum (121 MHz, C_6D_6) of the crude mixture obtained from the reaction of **2** and two equiv. PPh_3.

ii. Reaction of [^{i}Pr$_2$NN$_{F6}$]Cu(κ^2-O$_2$N) (3) with CNAr (Ar = 2,6-Me$_2$C$_6$H$_3$).

To a solution of **3** in C_6D_6 (2.0 mL of 15mM solution, 0.03 mmol) was added a C_6D_6 solution containing 2 equiv. 2,6-dimethylphenyl isocyanide (ArNC) (0.34 mL of 180 mM solution, 0.06 mmol). A trifluorotoluene standard was also added (1 equiv.). The color of the solution immediately changed from dark green to yellow with concomitant gas evolution (for gas trapping experiments see Section 12). After 4 h, the resultant solution was analyzed by ^{19}F NMR spectroscopy, which showed the formation of **6** in 52% yield as judged by the resonance at δ -64.18 ppm. ^{19}F NMR spectrum (376 MHz, C_6D_6): δ -66.50 (s, -C*F*$_3$, compound **1**), -64.18 (s, -C*F*$_3$, compound **6**). ^{1}H NMR (400 MHz, C_6D_6): δ 0.88 (t, 6H, Ar-C*H*$_3$, compound **6**), 1.34 (t, 24H, Ar-CH-(C*H*$_3$)$_2$, compound **6**), 3.33 (m, 4H, Ar-C*H*-(CH$_3$)$_2$, compound **6**), 6.25 (s, 1H, backbone-C*H*, compound **6**).

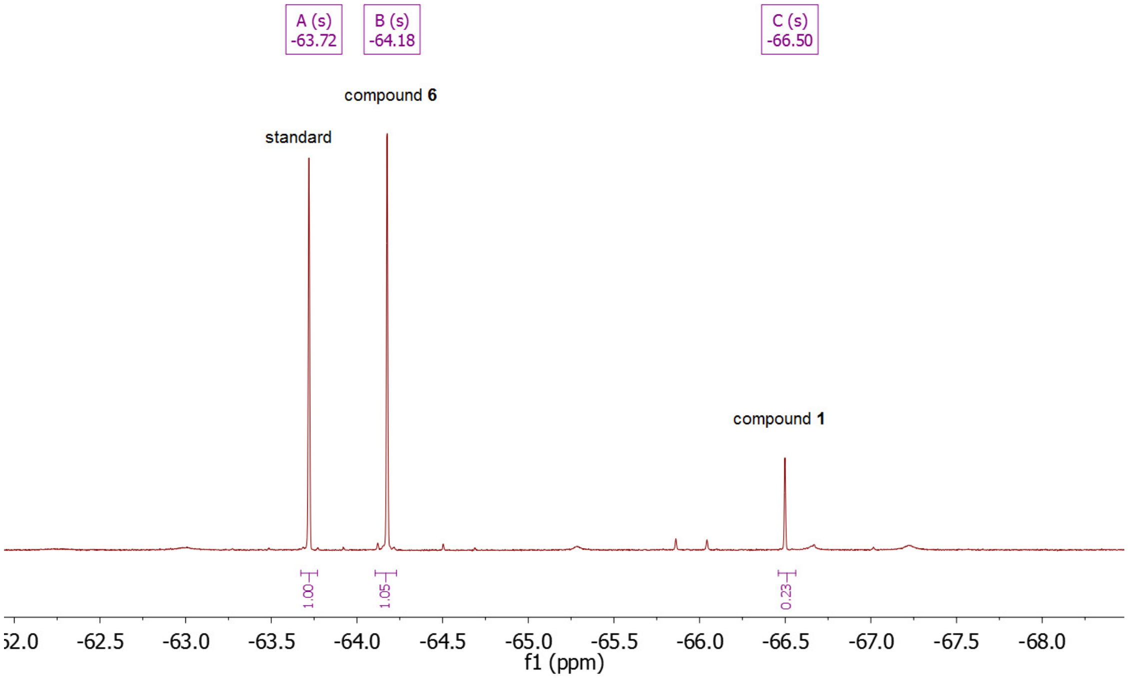

Figure S5. ^{19}F NMR spectrum (376 MHz, C_6D_6) of the crude mixture obtained from the reaction of **3** and two equiv. ArNC.

11. Reaction of $[Bu_4N]\{[^iPr_2NN_{F6}]Cu(\kappa^1\text{-}NO_2)\}$ (2) with PPh_3 and CNAr.

i. Reaction of $[Bu_4N]\{[^iPr_2NN_{F6}]Cu(\kappa^1\text{-}NO_2)\}$ (2) with PPh_3.

To a solution of **2** in C_6D_6 (1.5 mL of 30 mM solution, 0.045 mmol) was added a C_6D_6 solution of triphenylphosphine (0.38 mL of 120 mM solution, 0.045 mmol). A trifluorotoluene standard was also added (1 equiv). The color of the solution turned from deep red to pale orange over the course of 4 h after which time the resultant solution was analyzed by NMR spectroscopy, indicating the formation of **5** in 87% yield as judged by the resonance at δ -60.42 ppm. ^{19}F NMR spectrum (376 MHz, C_6D_6): *δ* -60.42 (s, -C*F*$_3$), -63.37 (s, -C*F*$_3$, unreacted **3**). ^1H NMR (400 MHz, C_6D_6): δ 0.73 (d, 12H, Ar-CH-(C*H*$_3$)$_2$), 1.27 (d, 12H, Ar-CH-(C*H*$_3$)$_2$), 3.39 (m, 4H, Ar-C*H*-(CH$_3$)$_2$), 6.24 (s, 1H, backbone-C*H*). ^{31}P NMR spectrum (121 MHz, C_6D_6): *δ* -8.36 (s, *P*Ph$_3$ unreacted), 0.11 (s, compound **5**).

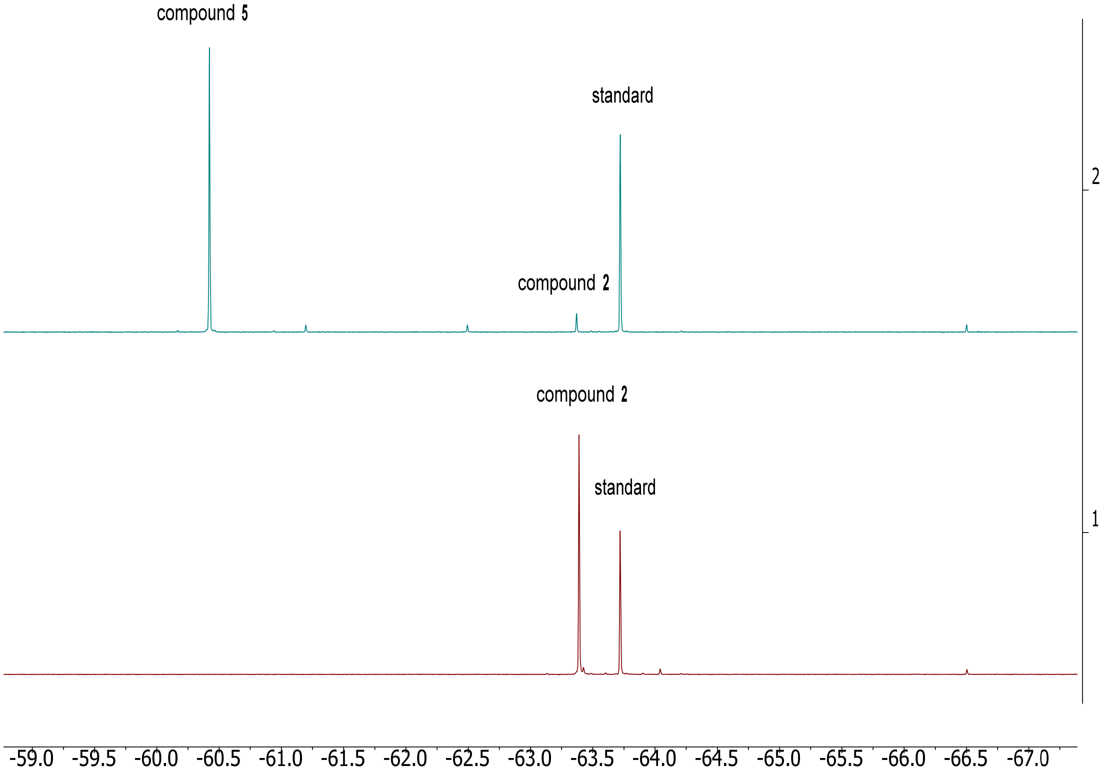

Figure S6. Comparison of ^{19}F NMR spectra (376 MHz, C_6D_6) of **2** (red trace) and crude mixture (green trace) obtained from the reaction between **2** and two equiv. PPh_3.

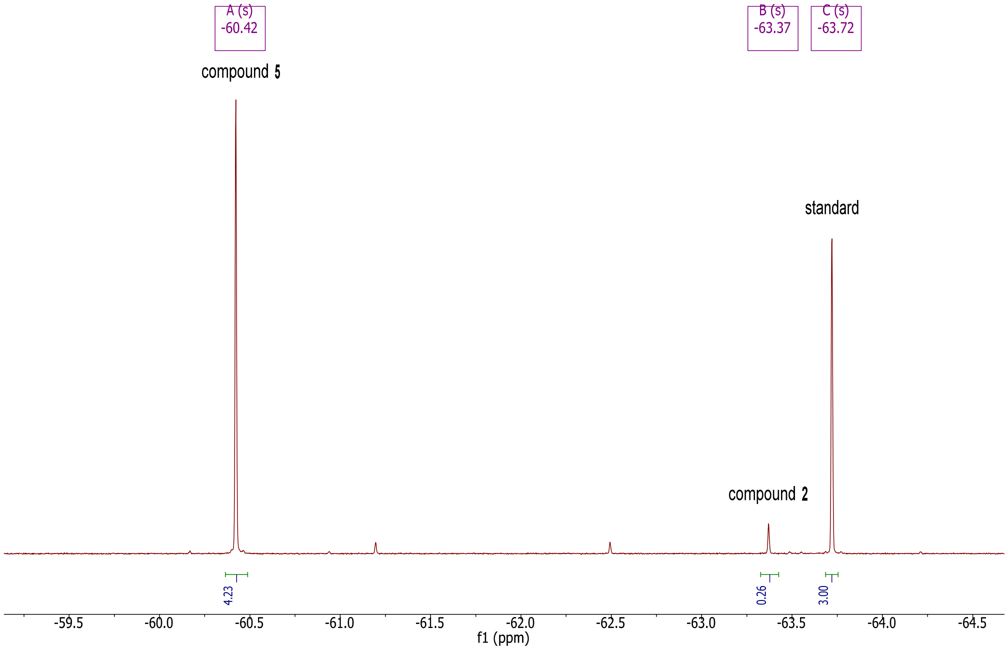

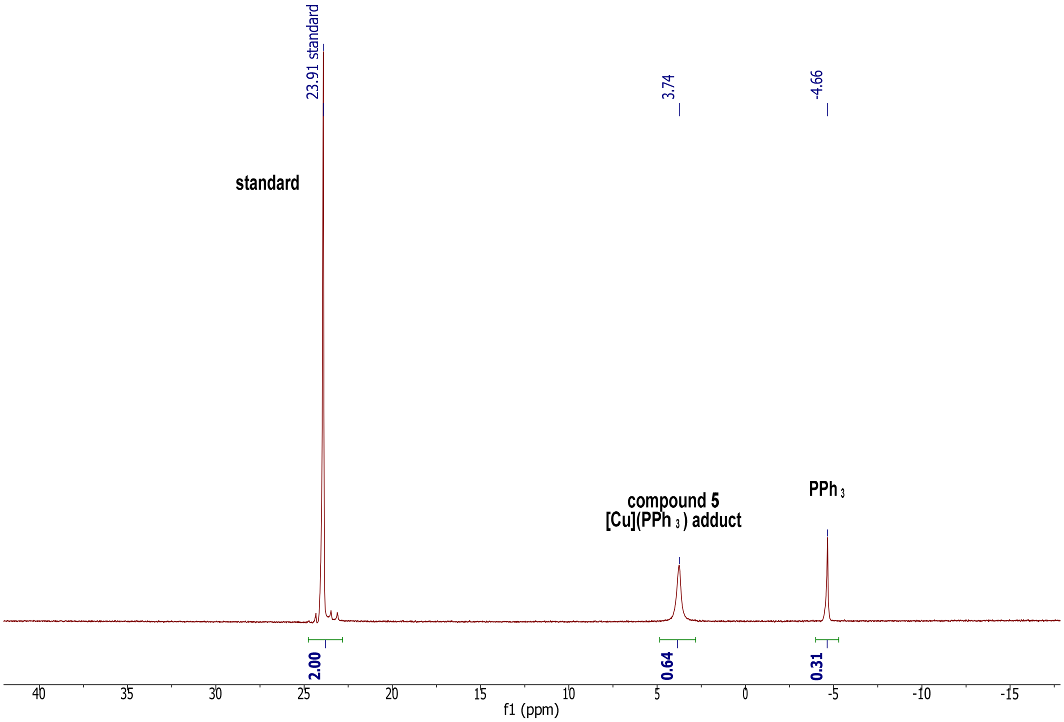

Figure S7. (top) ^{19}F NMR spectrum (376 MHz, C_6D_6) of the crude mixture obtained from the reaction of **2** and two equiv. PPh_3; (bottom) ^{31}P NMR spectrum (121 MHz, C_6D_6) of the crude mixture obtained from the reaction of **2** and two equiv. PPh_3.

ii. Reaction of [Bu$_4$N]{[^{i}Pr$_2$NN$_{F6}$]Cu(κ^1-NO$_2$)} (2) with CNAr.

To a solution of **2** in C_6D_6 (1.5 mL of a 30 mM solution, 0.045 mmol), a C_6D_6 solution of 2,6-dimethylphenyl isocyanide (0.25 mL of a 180 mM solution, 0.045 mmol) was added. A trifluorotoluene standard was also added (1 equiv). The color of the solution turned from deep red to pale orange over the course of 2 h after which the resultant solution was analyzed by NMR spectroscopy which showed the formation of **6** in 95% yield based on ^{19}F NMR. ^{19}F NMR spectrum (376 MHz, C_6D_6): *δ* -64.18 (s, -C*F*$_3$). ^{1}H NMR (400 MHz, C_6D_6): δ 0.98 (t, 12H, N-(CH$_2$)$_3$-C*H*$_3$), 1.34 (t, 24H, Ar-CH-(C*H*$_3$)$_2$), 1.49 (m, 8H, N-(CH$_2$)$_2$-C*H*$_2$-CH$_3$), 1.78 (s, 6H, Ar-C*H*$_3$), 3.24 (t, 8H, N-C*H*$_2$-C$_3$H$_7$), 3.33 (m, 4H, Ar-C*H*-(CH$_3$)$_2$), 6.25 (s, 1H, backbone-C*H*).

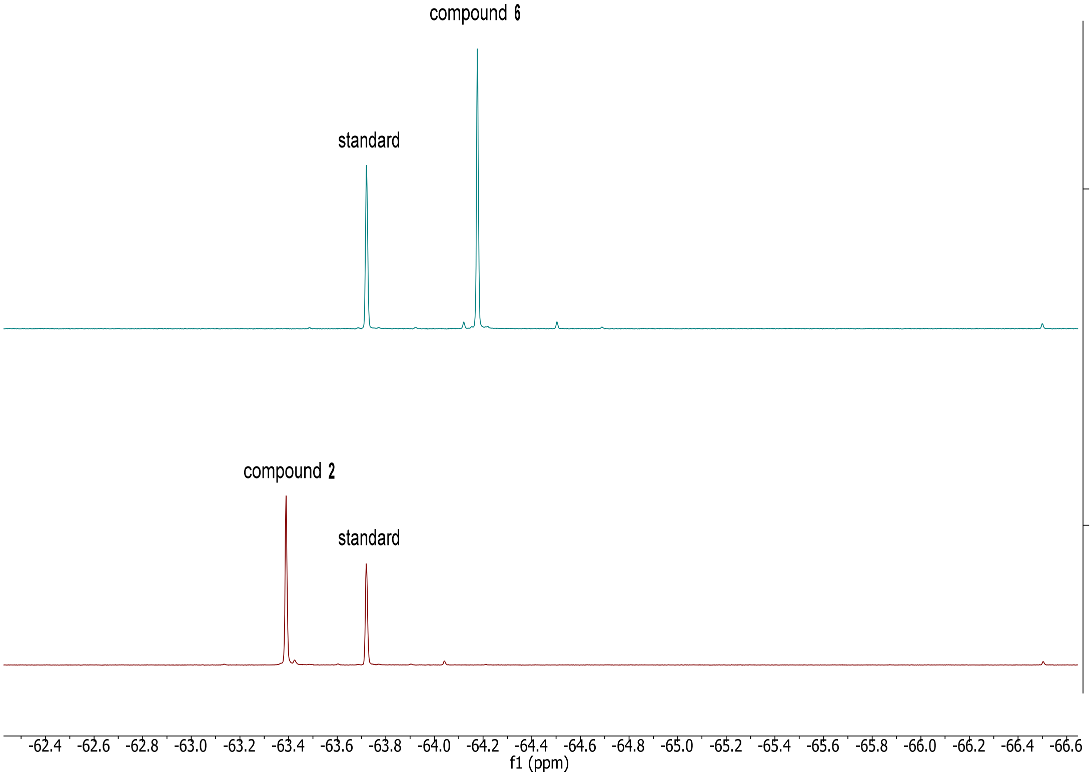

Figure S8. Comparison of ^{19}F NMR spectra (376 MHz, C_6D_6) of **2** (red trace) and crude mixture (green trace) obtained from the reaction between **2** and two equiv. CNAr.

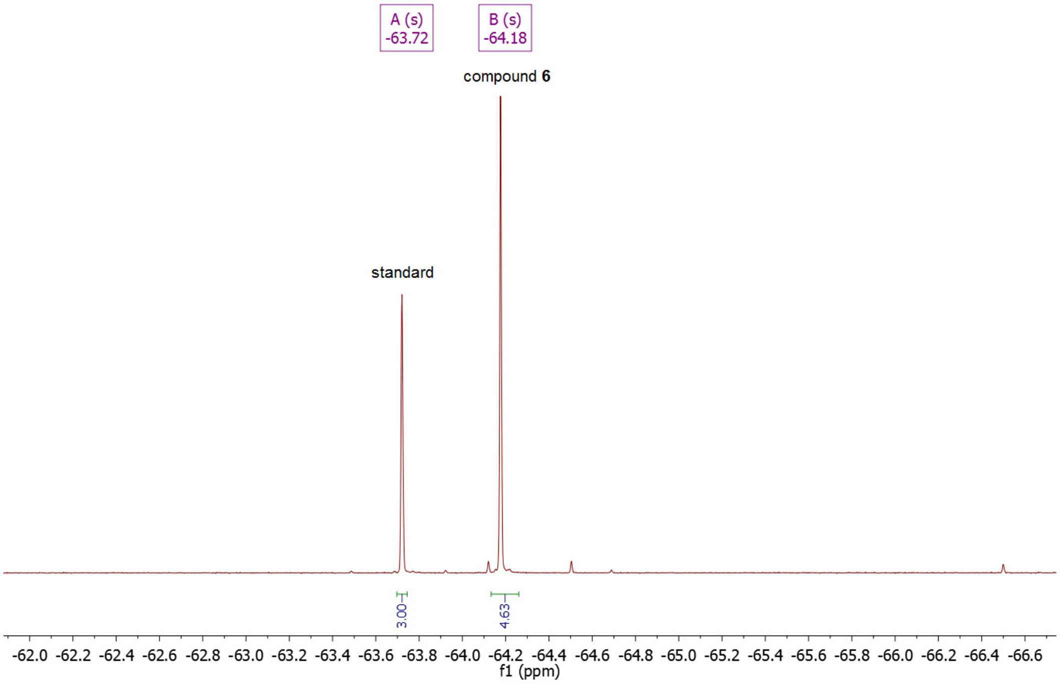

Figure S9. ^{19}F NMR spectrum (376 MHz, C_6D_6) of the crude mixture obtained from the reaction of **2** and two equiv. CNAr.

iii. Observation of nitrite by ^{15}N NMR spectroscopy.

Release of nitrite anion was also illustrated using **2-^{15}N**. A solution of **2-^{15}N** (0.65 mL of 150 mM solution, 0.097 mmol) in THF-*d*$_8$ was added to a solution of CNAr (0.65 mL of 180 mM solution, 0.097 mmol). The resultant orange solution was examined by ^{15}N NMR spectroscopy, indicating the formation of $[Bu_4N]^{15}NO_2$ as judged by the resonance at δ 617 ppm which corresponds to the free nitrite. The ^{15}N NMR spectrum of a separately synthesized $[Bu_4N]^{15}NO_2$ sample was obtained for comparison.

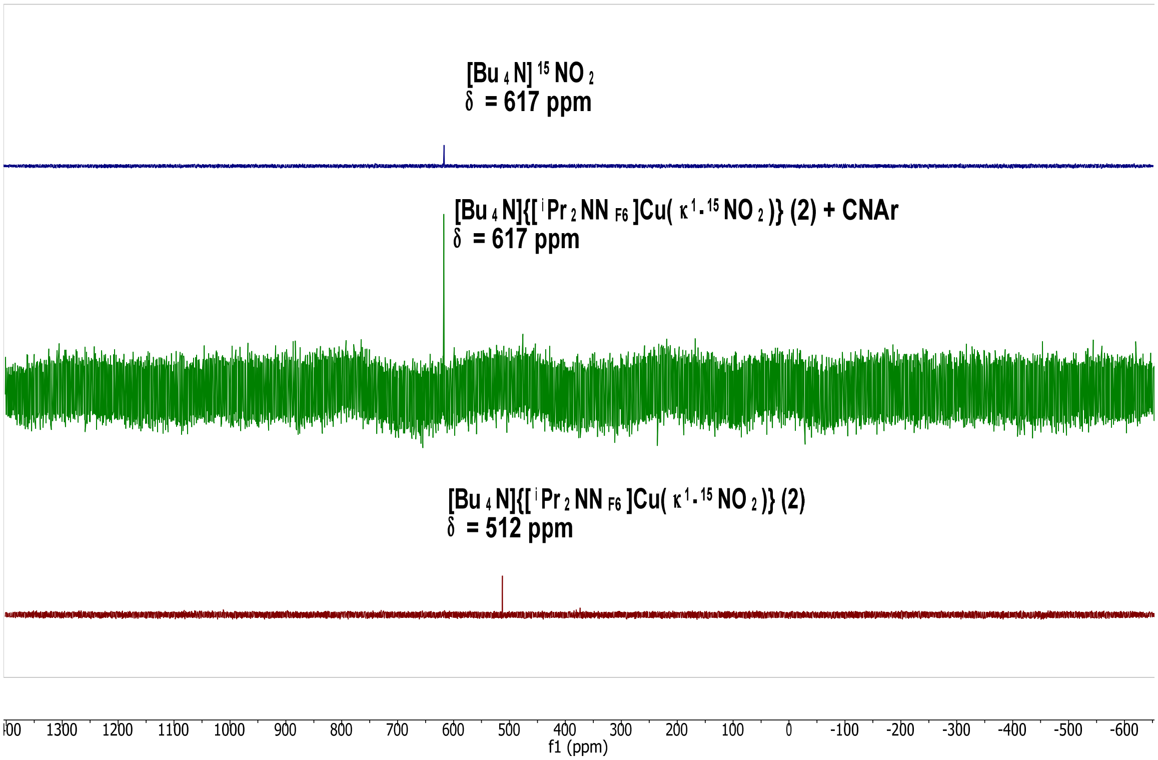

Figure S10. ^{15}N NMR spectrum (41 MHz, THF-*d*$_8$, RT) of (top) $[Bu_4N]^{15}NO_2$, (middle) the reaction of **2-^{15}N** and CNAr, (bottom) **2-^{15}N.**

12. Quantitative NO Trapping by (TPP)Co^{II} Complex.

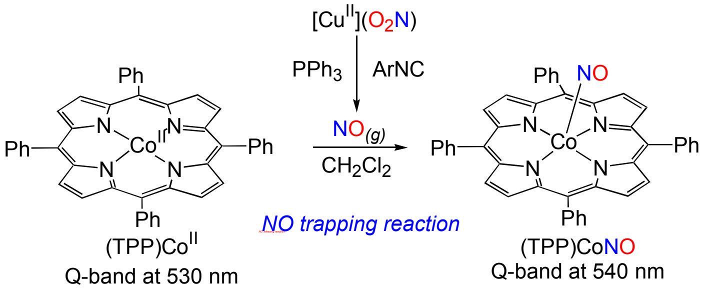

Scheme S3. Stoichiometric conversion of (TPP)Co^{II} to (TPP)Co(NO) utilized for NO quantification.

Figure S11. The setup for the NO quantification

(TPP)Co^{II} was used for quantitative trapping of nitric oxide using a similar experimental set up as previously demonstrated by Harrop.[4, 5] A smaller vial charged with a solution of **2** (1 mL 20 mM) in C_6H_6 was carefully placed in a larger vial containing a solution of (TPP)Co^{II} complex (20 mL, 1 mM) in CH_2Cl_2 and the bigger vial was sealed with a septum. A solution of triphenylphosphine (PPh_3) (0.5 mL 80 mM) in C_6H_6 was injected to the inner vial and solutions were stirred for 5 hr. Then an aliquot (100 µL) of the resultant (TPP)Co solution from the outer vial was diluted to 2 mL using CH_2Cl_2 and analyzed by UV-Vis spectroscopy. The Q-band absorption features in the UV-Vis spectra of authentic (TPP)Co^{II} (530 nm) and (TPP)Co(NO) (540 nm) samples were used to compare and quantify the yield of cobalt-nitrosyl species. The same experiment was performed on the reaction of **2** with 2 equiv. 2,6-dimethylphenyl isocyanide (ArNC).

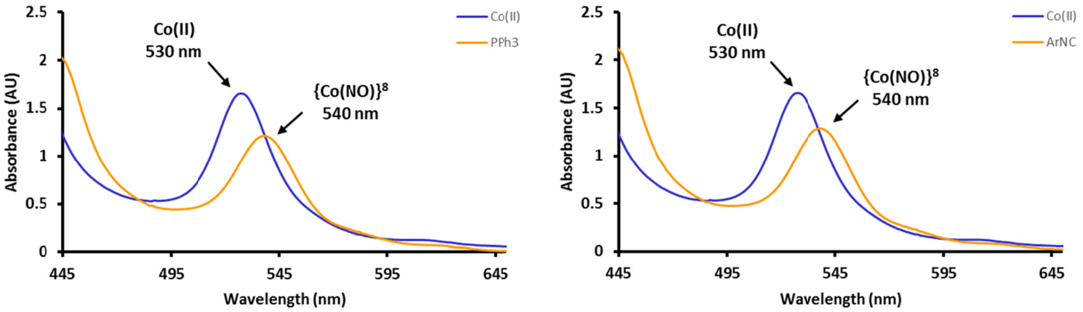

Figure S12. UV-Vis spectra (in CH_2Cl_2 at 25 °C) of (TPP)Co (blue trace) and (TPP)Co(NO) species generated upon reacting (TPP)Co with NO released from the mixture of **2** and (left) PPh_3 and (right) ArNC (orange trace).

13. EPR Spectroscopy of 3 and 4.

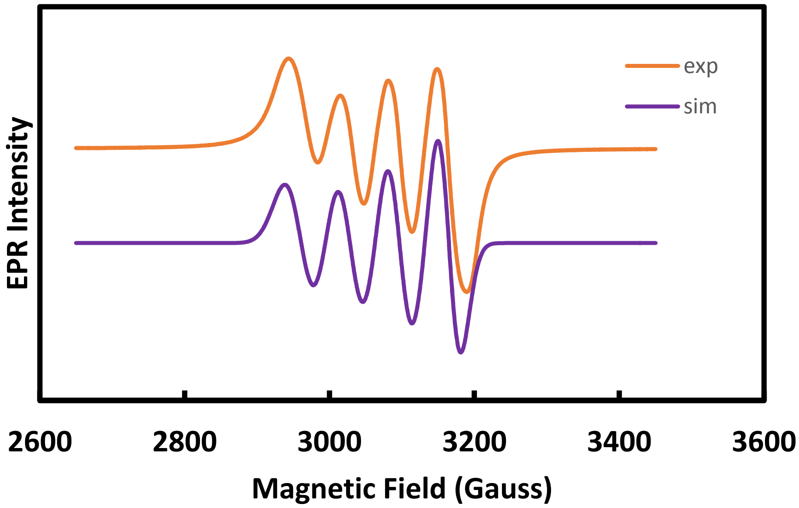

Figure S13. Isotropic X-band electron paramagnetic resonance (EPR) spectrum and simulation for [^{i}Pr$_2$NN$_{F6}$]Cu(κ^2-O$_2$N) (**3**) (4.0 mM in pentane at 293 K). Frequency = 8.995450 GHz, Power = 1 mW, ModWidth = 0.4 mT, time constant = 0.1 s. Simulation was performed using 1Cu, 2N model: g_{iso} = 2.098, A_{Cu} = 205 MHz, A_{2N} = 36 MHz.

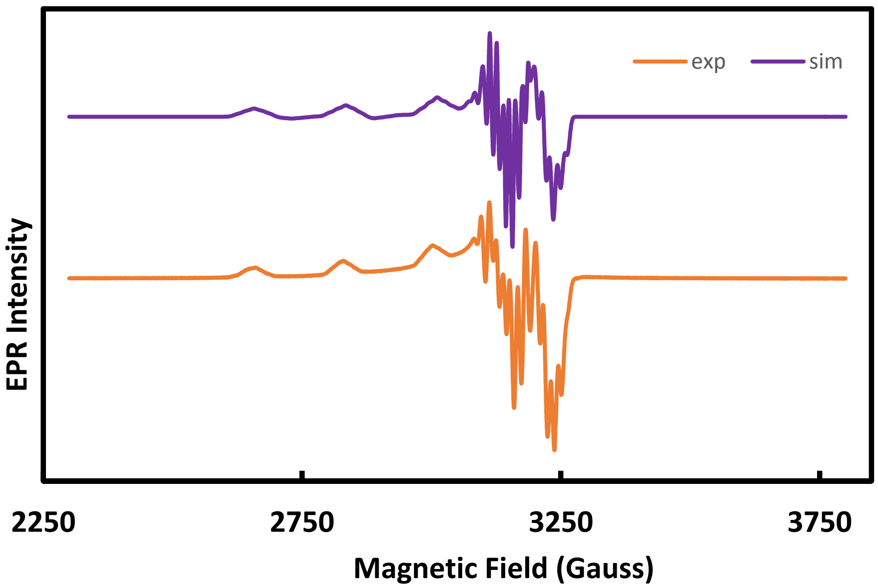

Figure S14. Anisotropic X-band electron paramagnetic resonance (EPR) spectrum and simulation for [$^{i}\mathrm{Pr}_2\mathrm{NN}_{\mathrm{F6}}$]Cu($\kappa^2$-$\mathrm{O_2N}$) (**3**) (4.0 mM in pentane at 80 K). Frequency = 8.996813 GHz, Power = 1 mW, ModWidth = 0.4 mT, time constant = 0.1 s. Simulation was performed using 1Cu, 2N model: $g_{\perp}$ = 2.0515, $g_{\parallel}$ = 2.199, $A_{\perp}(^{14}\mathrm{N})$ = 39 MHz , $A_{\parallel}(^{14}\mathrm{N})$ = 49 MHz, $A_{\perp}(^{63/65}\mathrm{Cu})$ = 35 MHz , $A_{\parallel}(^{63/65}\mathrm{Cu})$ = 545 MHz.

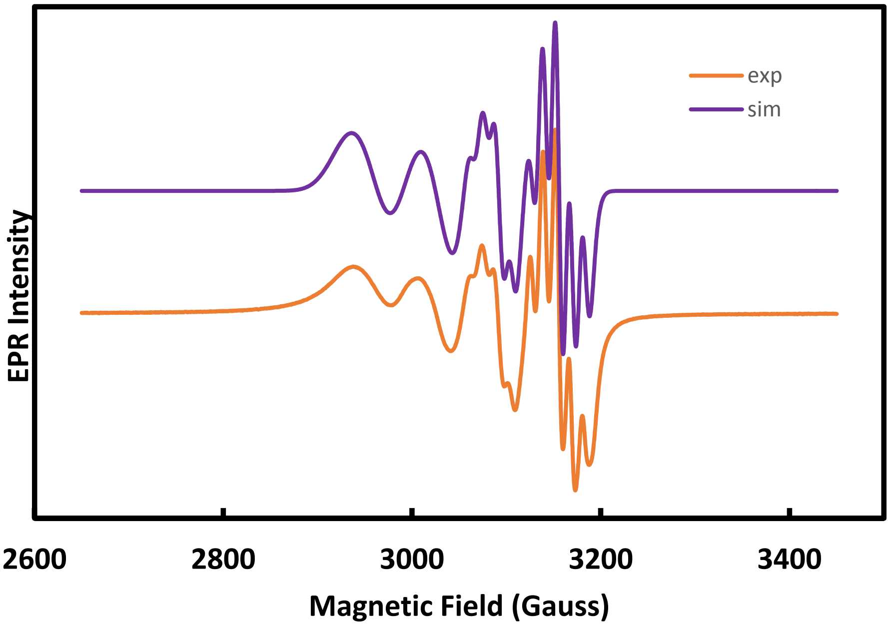

Figure S15. Isotropic X-band electron paramagnetic resonance (EPR) spectrum and simulation for $\{[^{i}Pr_2NN_{F6}]Cu1_2(\mu\text{-}\kappa^2\text{:}\kappa^1\text{-}O_2N)$ (**4**) (4.0 mM in pentane at 293 K). Frequency = 8.995450 GHz, Power = 1 mW, ModWidth = 0.4 mT, time constant = 0.1 s. Simulation was performed using 1Cu, 2N model: $g_{iso} = 2.100$, $A_{Cu} = 190$ MHz, $A_{2N} = 40$ MHz.

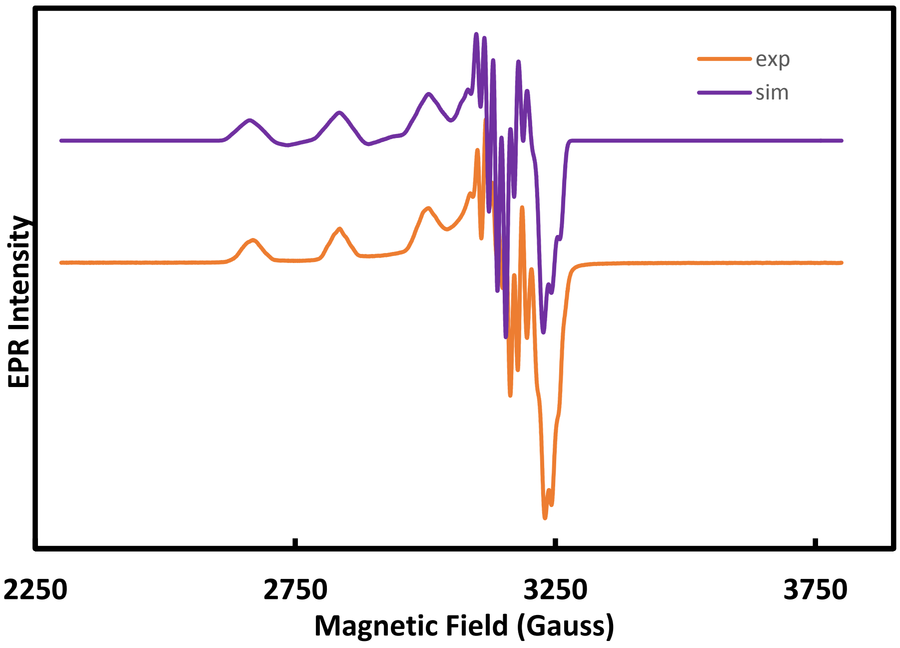

Figure S16. Anisotropic X-band electron paramagnetic resonance (EPR) spectrum and simulation for $\{[^{i}Pr_2NN_{F6}]Cu\}_2(\mu\text{-}\kappa^2\text{:}\kappa^1\text{-}O_2N)$ (**4**) (4.0 mM in pentane at 80 K). Frequency = 8.995450 GHz, Power = 1 mW, ModWidth = 0.4 mT, time constant = 0.1 s. Simulation was performed using 1Cu, 2N model: $g_{\perp} = 2.050$, $g_{\parallel} = 2.200$, $A_{\perp}(^{14}N) = 48$ MHz , $A_{\parallel}(^{14}N) = 49$ MHz, $A_{\perp}(^{63/65}Cu) = 35$ MHz , $A_{\parallel}(^{63/65}Cu) = 530$ MHz.

14. Cyclic Voltammetry of 2, 3 and 4.

The cyclic voltammetry of **2**, **3** and **4** was performed on a 1.0 mM solution of the compound in THF using $[Bu_4N]PF_6$ electrolyte. Platinum working electrode, platinum wire auxiliary electrode, $Ag/AgNO_3$ reference electrode and 20-50 mVs^{-1} scan rate were used for CV.

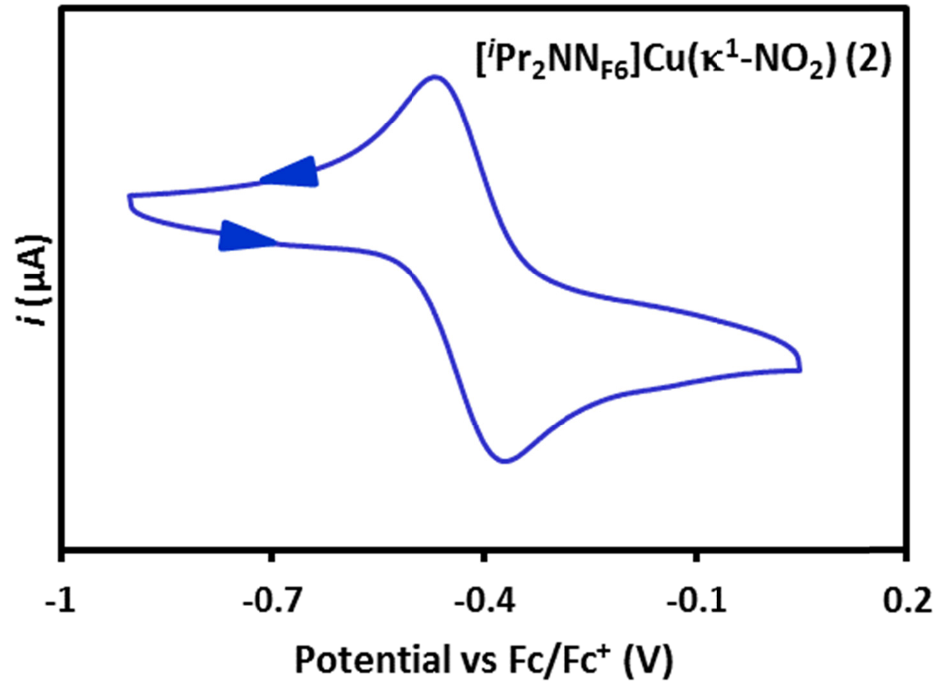

Figure S17. Cyclic voltammogram of $[^iPr_2NN_{F6}]Cu(\kappa^1\text{-}NO_2)$ (**2**) (1.0 mM in THF at 25 °C) in presence of *n*-tetrabutylammonium hexafluorophosphate (0.1 M). Scan proceeds at the rate of 50 mV/s. $E_{1/2}$ = -420 mV; ΔE = 99 mV.

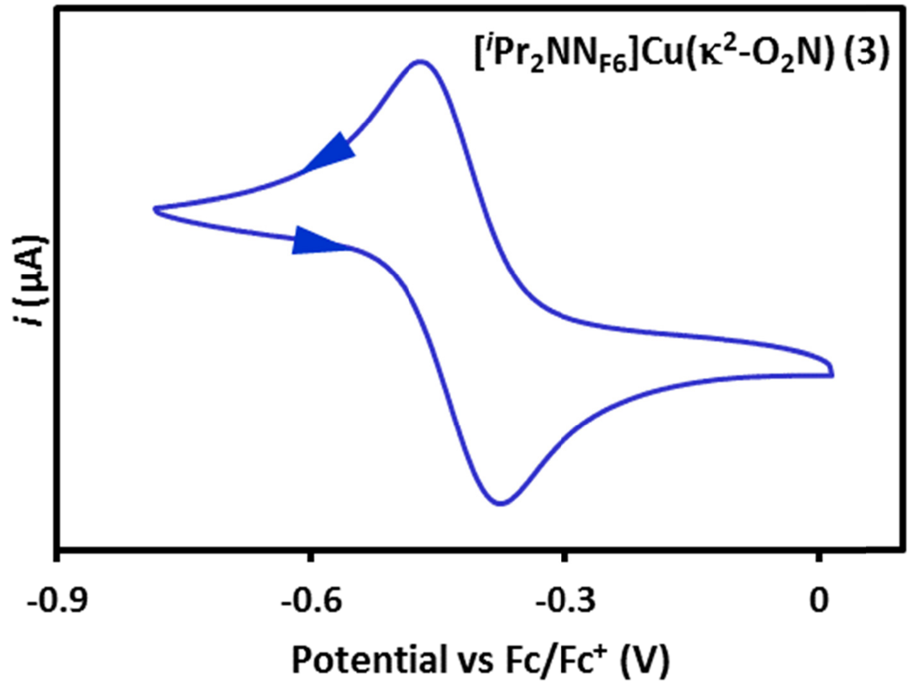

Figure S18. Cyclic voltammogram of [^{i}Pr$_2$NN$_{F6}$]Cu(κ^2-O$_2$N) (**3**) (1.0 mM in THF at 25 °C) in presence of *n*-tetrabutylammonium hexafluorophosphate (0.1 M). Scan proceeds at the rate of 20 mV/s. $E_{1/2}$ = -420 mV; ΔE = 99 mV.

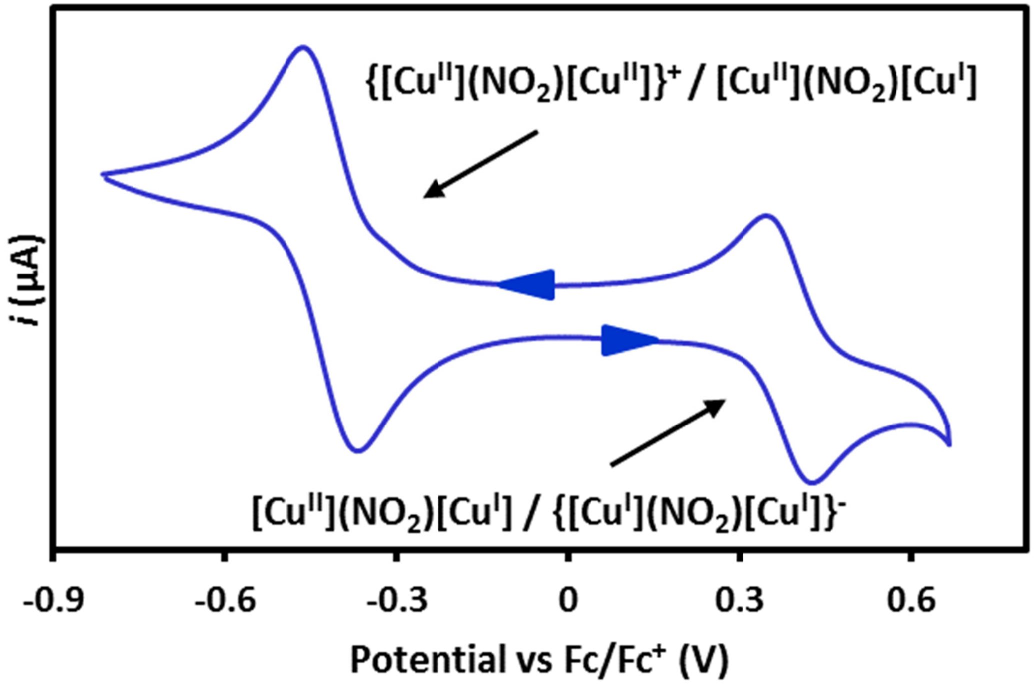

Figure S19. Cyclic voltammogram of $\{[^i\mathrm{Pr}_2\mathrm{NN}_{\mathrm{F6}}]\mathrm{Cu}\}_2(\mu\text{-}\kappa^2\text{:}\kappa^1\text{-O}_2\mathrm{N})$ (**4**) (1.0 mM in THF at 25 °C) in presence of *n*-tetrabutylammonium hexafluorophosphate (0.1 M). Scan proceeds at the rate of 50 mV/s.

$E_{1/2}$ = -413 mV; ΔE = 94 mV ([Cu^{II}](NO$_2$)[Cu^I] / {[Cu^I](NO$_2$)[Cu^I]}$^-$)

$E_{1/2}$ = 385 mV; ΔE = 80 mV ({[Cu^{II}](NO$_2$)[Cu^{II}]}$^+$ / [Cu^{II}](NO$_2$)[Cu^I])

References for synthetic and experimental details

1. R. E. Weston JR., T. F. Brodasky, *J. Chem. Phys.*, 1957, **27**, 683-689.
2. D. T. Carey, E. K. Cope-Eatough, E. Vilaplana-Mafe, F. S. Mair, R. G. Pritchard, J. E. Warren and R. J. Woods, *Dalton Trans.*, 2003, DOI: 10.1039/b212079h, 1083-1093.
3. M. D. Lim, I. M. Lorkovic and P. C. Ford, *Inorg. Chem.*, 2002, **41**, 1026-1028.
4. B. C. Sanders, S. M. Hassan and T. C. Harrop, *J. Am. Chem. Soc.*, 2014, **136**, 10230-10233.
5. M. Kumar, N. A. Dixon, A. C. Merkle, M. Zeller, N. Lehnert and E. T. Papish, *Inorg. Chem.*, 2012, **51**, 7004-7006.

15. Crystallographic Details

Single crystals of compound **1** (CCDC 1511514), **2** (CCDC 1511515), **3** (CCDC 1511519), **4** (CCDC 1511516), **5** (CCDC 1511517), and **6** (CCDC 1511518) were mounted under mineral oil or perfluoroalkyl ether oil on a Mitegen Micromount in a cold nitrogen stream at 100(2) K. Data for compound **6** was collected on a Bruker D8 Quest equipped with a Photon100 CMOS detector and a Mo ImS source. Data for compounds **1**, **2**, **3**, **4** and **5** were collected on a Bruker DUO equipped with an APEXII CCD detector and Mo fine-focus sealed source. Either full spheres (triclinic) or hemispheres (monoclinic or higher) of data were collected (0.3° or 0.5° ω-scans; $2\theta_{max} \geq 50°$; monochromatic Mo Ka radiation, λ = 0.7107 Å) depending on the crystal system and integrated with the Bruker SAINT program. Structure solutions were performed using the SHELXTL/PC suite[a] and XSEED[b]. Intensities were corrected for Lorentz and polarization effects and an empirical absorption correction was applied using Blessing's method as incorporated into the program SADABS.[c] Non-hydrogen atoms were refined with anisotropic thermal parameters and hydrogen atoms were included in idealized positions. Structures were rendered with POV-Ray in XSEED using 50% probability ellipsoids. Further comments on disorder models:

[^{i}Pr$_2$NN$_{F6}$]Cu(η^2-benzene) (1): One CF_3 group is disordered over two positions. The like C-C and C-F distances were restrained to be similar (esd 0.01Å). The F•••F distances were restrained to be similar (esd 0.02Å).

[^{i}Pr$_2$NN$_{F6}$]Cu(κ^1-NO$_2$) (2): There are two ion pairs per asymmetric unit. One aryl group on anion one is disordered over two positions. The like Cu-N, N-C, and C-C distances were restrained to be similar (esd 0.01Å). Two isopropyl group on anion one are disordered over two positions. The like C-C distances were restrained to be similar (esd 0.01Å). One CF_3 group on anion one is disordered over two positions. The like C-C and C-F distances were restrained to be similar (esd 0.01Å). The F•••F distances were restrained to be similar (esd 0.02Å). Two butyl groups of cation one are disordered over two positions. The like N-C and C-C distances were restrained to be similar (esd 0.01Å). One butyl group of cation two is disordered over two positions. The like N-C and C-C distances were restrained to be similar (esd 0.01Å). Two reflections were omitted from the final refinement because they were partially obscured by the shadow of the beam stop.

[^{i}Pr$_2$NN$_{F6}$]Cu(κ^2-O$_2$N) (3): The datum crystal of (3) was twinned. The twin law by rows relating the primary domain to the secondary domain is (1 -0.5 0), (0 -1 0), (0 0 -1). The ratio of the twin domains refines to approximately 63% : 37%.

{[^{i}Pr$_2$NN$_{F6}$]Cu}(μ-κ^2:κ^1-NO$_2$) (4): One half of the molecule is present in the asymmetric unit, the other half is generated by the symmetry operation [-x+1, y, -z+3/2]. Four highly disordered fluorobenzene solvent molecules were also present. Attempts to model these disordered solvent molecules were unsuccessful and so they were removed from the model using the squeeze routine in PLATON.[d] The electron count from the squeeze model is in good agreement with the electron count predicted from the solvent molecules. The bridging NO_2 group is disordered across the symmetry site over two orientations. The major orientation is Cu1••• (μ-κ^2:κ^1-NO$_2$) •••Cu1' and the minor orientation is Cu1••• (μ-κ^1:κ^2-NO$_2$) •••Cu1' where Cu1' is generated by the symmetry operation [-x+1, y, -z+3/2]. The NO_2 nitrogen atoms of each orientation (N3/N3B) were constrained to have equal x,y,z positions as well as equal anisotropic displacement parameters. The like Cu-O and N-O distances were restrained to be similar (esd 0.01Å).

[^{i}Pr$_2$NN$_{F6}$]Cu(PPh$_3$) (5): There are two molecules in the asymmetric unit along with three highly disordered pentane solvent molecules. Attempts to model these disordered solvent molecules were unsuccessful and so they were removed from the model using the squeeze routine in PLATON. The electron count from the squeeze model is in good agreement with the electron count predicted from the solvent molecules. One CF_3 group on molecule one is disordered over two positions. The C-F distances were restrained to be similar (esd 0.01Å). The F•••F distances were restrained to be similar (esd 0.02Å). One of the aryl groups on molecule one is disordered over two positions. The like C-C and C-N distances were restrained to be similar (esd 0.01Å). One CF_3 group on molecule two is disordered over two positions. The like C-C and C-F distances were restrained to be similar (esd 0.01Å). The F•••F distances were restrained to be similar (esd 0.02Å).

One isopropyl group of molecule two is disordered over two positions. The like C-C distances were restrained to be similar (esd 0.01Å).

[^{i}Pr$_2$NN$_{F6}$]Cu(CNAr) (6): There are two molecule in the asymmetric unit along with one toluene solvent molecule. The toluene is disordered over two positions. The like C-C distances were restrained to be similar (esd 0.01Å).

References for crystal structure refinements.

(a) SHELXTL-PC, Vers. 5.10; 1998, Bruker-Analytical X-ray Services, Madison, WI; G. M. Sheldrick, SHELX-97, Universität Göttingen, Göttingen,Germany.
(b) L. Barbour, XSEED, 1999.
(c) SADABS; G. M. Sheldrick, 1996, based on the method described in R. H. Blessing, *Acta Crystallogr. Sect. A*, **1995**, 51, 33.
(d) Spek, A. L., Structure validation in chemical crystallography. *Acta. Crystallogr. Sect. D Biol. Crystallogr.* **2009,** *65* (Pt 2), 148-55.

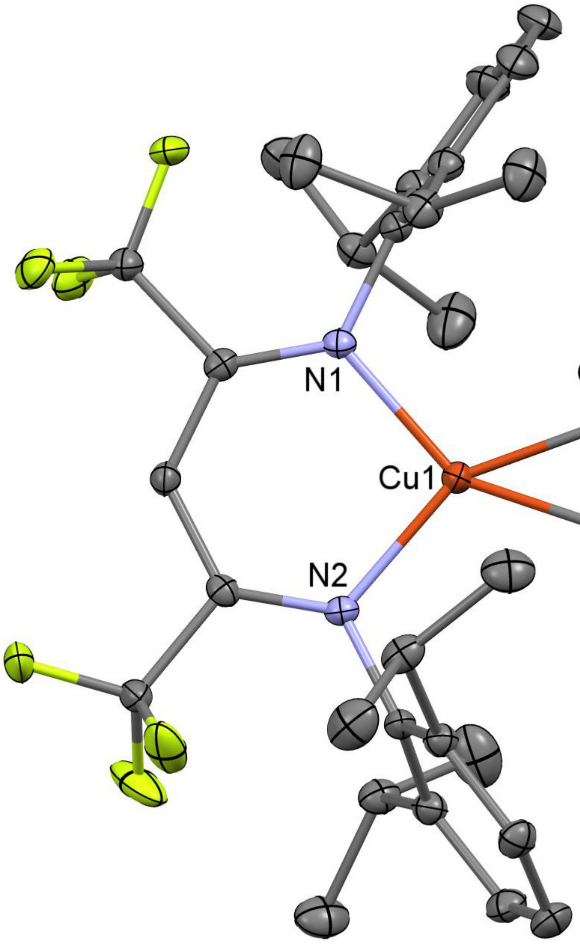

Figure S20. Molecular structure of [${}^{i}Pr_2NN_{F6}$]Cu(η^2-benzene) (**1**) (CCDC 1511514). Thermal ellipsoid plots are shown at 50% probability level and hydrogen atoms are omitted for clarity. Only the major component of disordered sites is shown. Selected bond distances (Å) and angles (deg): Cu1-C30 2.1259(15), Cu-C31 2.1512(15), Cu1-N1 1.9639(12), Cu1-N2 1.9526(12), C30-Cu1-C31 38.36(6).

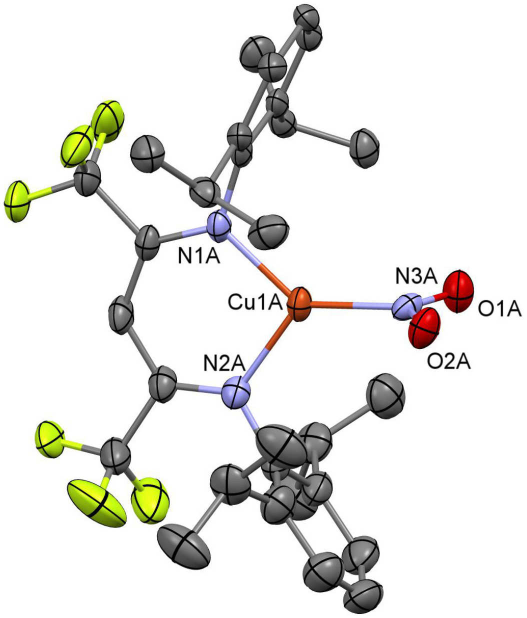

Figure S21. Molecular structure of molecule A of $[^{i}Pr_2NN_{F6}]Cu(\kappa^1\text{-}NO_2)$ (**2**) (CCDC 1511515); Molecule A. Thermal ellipsoid plots are shown at 50% probability level and hydrogen atoms are omitted for clarity. Tetrabutylammonium cation is omitted for clarity. Only the major component of disordered sites is shown. Selected bond distances (Å) and angles (deg): Cu1A-N1A 1.942(2), Cu1A-N2A 1.975(2), Cu1A-N3A 1.923(2), N3A-O1A 1.208(3), N3A-O2A 1.251(2), O1A-N3A-O2A 119.0(2).

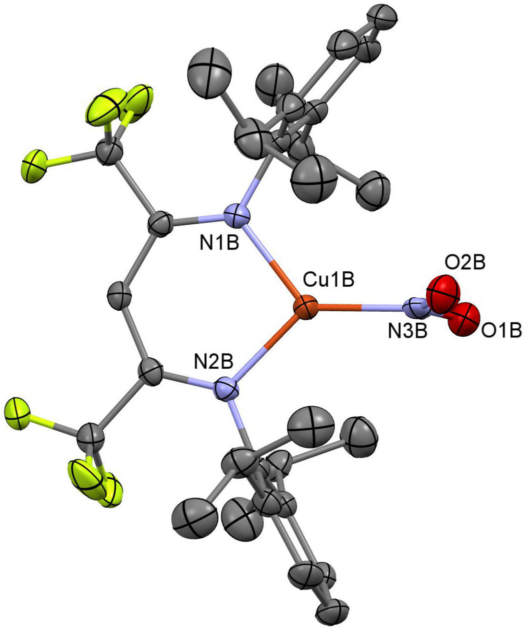

Figure S22. Molecular structure of molecule B of $[^{i}Pr_2NN_{F6}]Cu(\kappa^1\text{-}NO_2)$ (**2**) (CCDC 1511515); Molecule B. Thermal ellipsoid plots are shown at 50% probability level and hydrogen atoms are omitted for clarity. Tetrabutylammonium cation is omitted for clarity. Only the major component of disordered sites is shown. Selected bond distances (Å) and angles (deg): Cu1B-N1B 1.9557(17), Cu1B-N2B 1.9473(18), Cu1B-N3B 1.920(2), N3B-O1B 1.191(3), N3B-O2B 1.264(3), O1B-N3B-O2B 119.2(2).

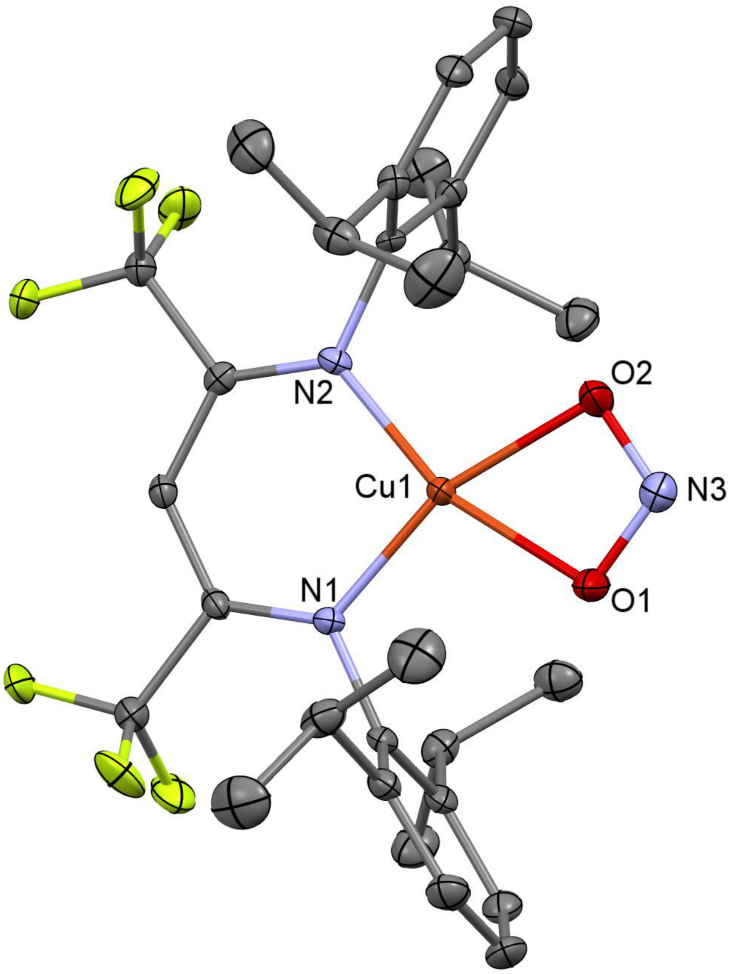

Figure S23. Molecular structure of $[^{i}Pr_2NN_{F6}]Cu(\kappa^2\text{-}O_2N)$ (**3**) (CCDC 1511519). Thermal ellipsoid plots are shown at 50% probability level and hydrogen atoms are omitted for clarity. Selected bond distances (Å) and angles (deg): Cu1-N1 1.901(2), Cu1-N2 1.900(2), Cu1-O1 2.0286(19), Cu1-O2 2.0126(19), N3-O1 1.259(3), N3-O2 1.263(3), O1-N3-O2 109.61(18), O1-Cu1-O2 61.32(7).

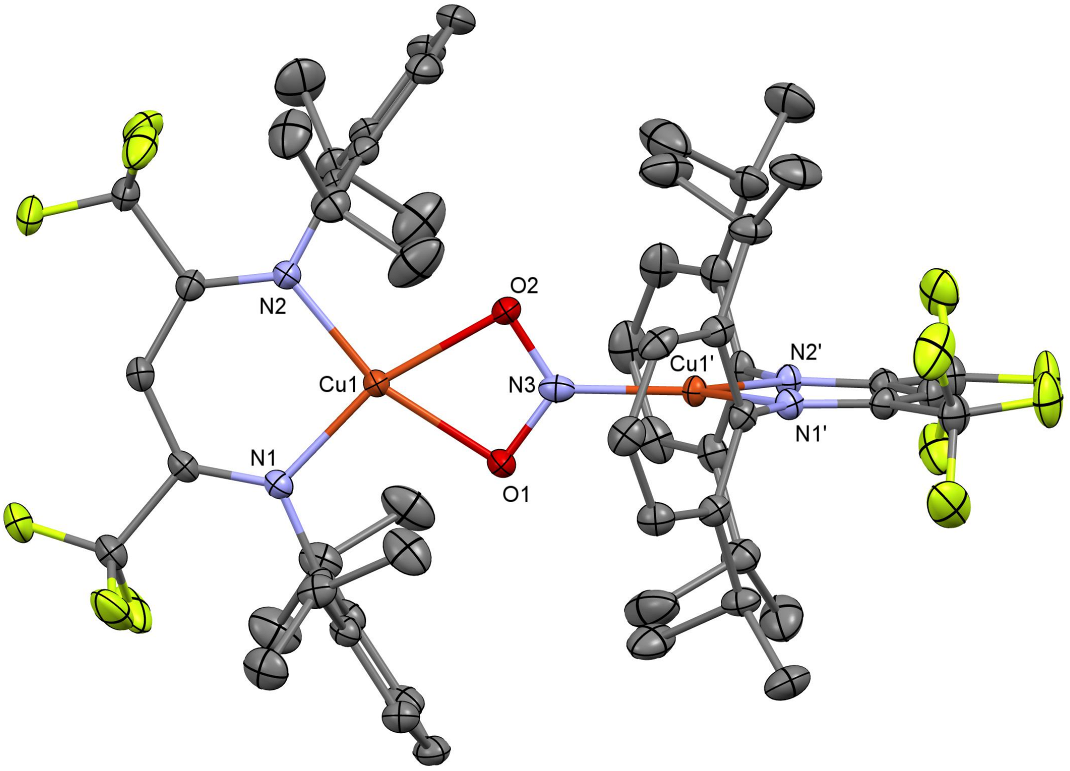

Figure S24. Molecular structure of $\{[^{i}\mathrm{Pr}_2\mathrm{NN}_{\mathrm{F6}}]\mathrm{Cu}\}(\mu\text{-}\kappa^2\text{:}\kappa^1\text{-}\mathrm{NO}_2)$ (**4**) (CCDC 1511516). Thermal ellipsoid plots are shown at 50% probability level and hydrogen atoms are omitted for clarity. Only the major component of disordered sites is shown. Symmetry operation [-x+1, y, -z+3/2]. Selected bond distances (Å) and angles (deg): Cu1-N1 1.9216(12), Cu1-N2 1.9196(12), Cu1-O1B 2.029(9), Cu1-O2B 2.029(9), N3-O1 1.274(4), N3-O2 1.274(3), O1-N3-O2 110.9(2), Cu1'-N3.

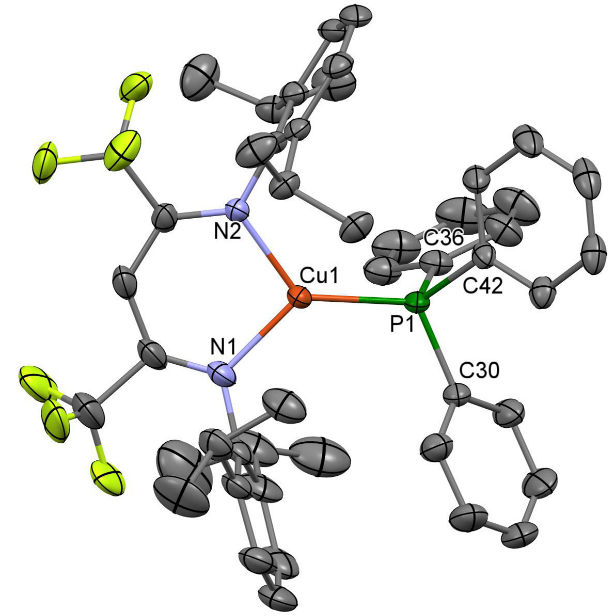

Figure S25. Molecular structure of molecule 1 of [^{i}Pr$_2$NN$_{F6}$]Cu(PPh$_3$) (**5**) (CCDC 1511517). Thermal ellipsoid plots are shown at 50% probability level and hydrogen atoms are omitted for clarity. Only the major component of disordered sites is shown. Selected bond distances (Å) and angles (deg): Cu1-N1 1.9793(13), Cu1-N2 1.9794(12), Cu1-P1 2.1922(4), P1-C30 1.8253(15), P1-C36 1.8205(17), P1-C42 1.8304(15).

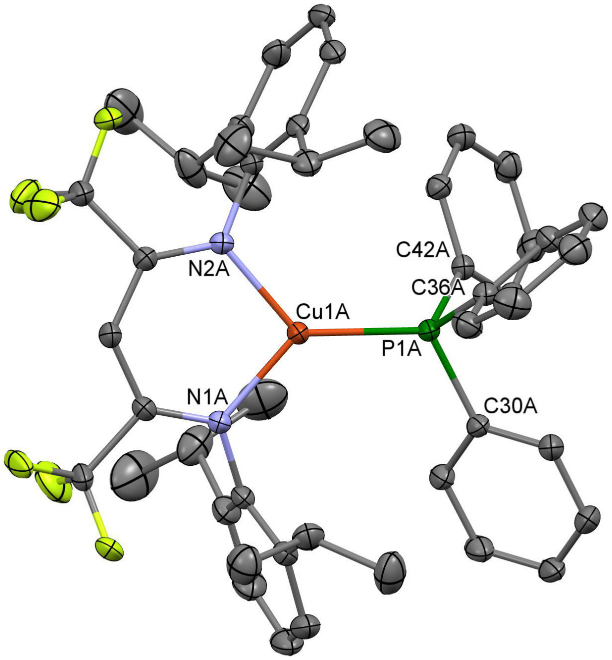

Figure S26. Molecular structure of molecule 2 of [^{i}Pr$_2$NN$_{F6}$]Cu(PPh$_3$) (**5**) (CCDC 1511517). Thermal ellipsoid plots are shown at 50% probability level and hydrogen atoms are omitted for clarity. Only the major component of disordered sites is shown. Selected bond distances (Å) and angles (deg): Cu1A-N1A 1.9819(11), Cu1A-N2A 1.9933(11), Cu1A-P1A 2.1971(4), P1A-C30A 1.8272(13), P1A-C36A 1.8307(14), P1A-C42A 1.8309(14).

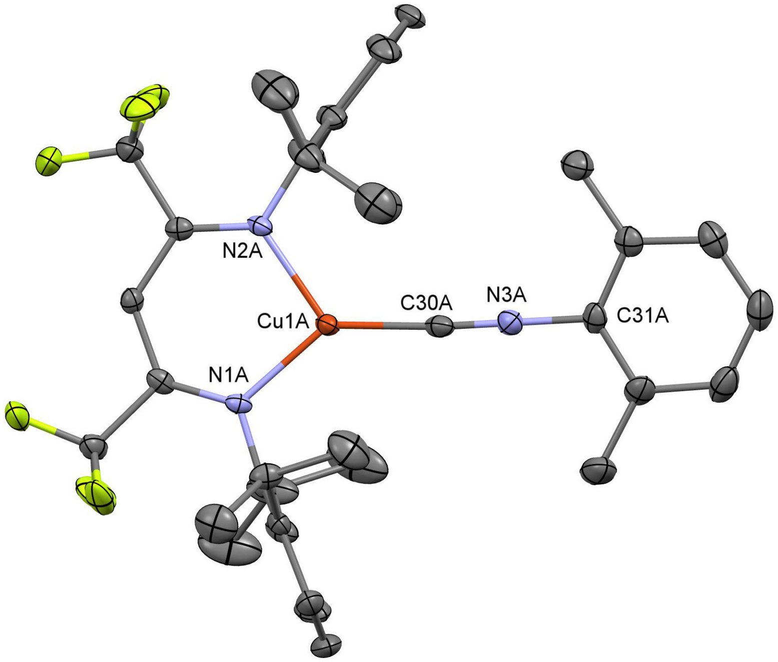

Figure S27. Molecular structure of molecule A of [^{i}Pr$_2$NN$_{F6}$]Cu(CNAr) (**6**) (CCDC 1511518). Thermal ellipsoid plots are shown at 50% probability level and hydrogen atoms are omitted for clarity. Only the major component of disordered sites is shown. Selected bond distances (Å) and angles (deg): Cu1A-N1A 1.9383(15), Cu1A-N2A 1.9555(15), Cu1A-C30A 1.828(2), C30A-N3A 1.158(2), N3A-C31A 1.401(2).

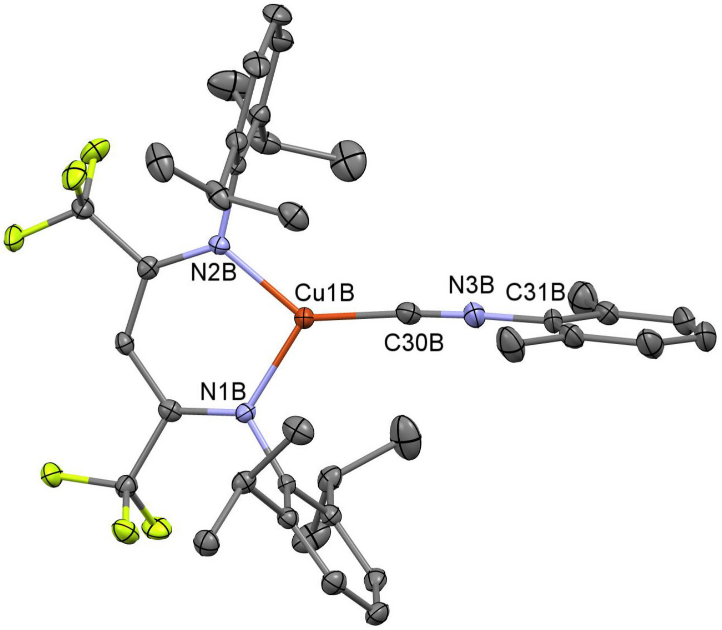

Figure S28. Molecular structure of molecule B of [^{i}Pr$_2$NN$_{F6}$]Cu(CNAr) (**6**) (CCDC 1511518). Thermal ellipsoid plots are shown at 50% probability level and hydrogen atoms are omitted for clarity. Only the major component of disordered sites is shown. Selected bond distances (Å) and angles (deg): Cu1B-N1B 1.9618(14), Cu1B-N2B 1.9427(14), Cu1B-C30B 1.830(2), C30B-N3B 1.159(2), N3B-C31B 1.405(2).